JOURNAL OF SCIENTIFIC RESEARCH
Department of Pure and Applied Chemistry
Faculty of Science
University of Maiduguri

TWO-PATCH SIS STOCHASTIC MODEL: EFFECTS OF DISPERSAL RATES ON DISEASE TRANSMISSION

[1]Auwal Abdullahi and [2]Babale Aliyu

*[1]Department of Mathematics and Computer Science, Federal University Kashere, Nigeria

[2]Department of Botany, Faculty of Science, Gombe State University, Nigeria
*Corresponding Email Address: auwal.abdullahi247@gmail.com

ABSTRACT

Communicable diseases including measles, Covid-19 and Ebola virus can be transmitted from one community to the other through epidemic dispersal. Different dispersal mechanisms were investigated using a verity of mathematical models; however, the effect of dispersal rates on diseases transmitting between communities that differ in healthcare provisions has not been previously studied. This study, therefore, investigated such effects on the transmission of infectious diseases between two distinct patches: a community with (without) better healthcare facilities. The stochastic susceptible-infected-susceptible (SIS) model, devised through the continuous-time Markov chain (CTMC) process, together with its corresponding ordinary differential equation (ODE) model, was used to determine how changes in dispersal rates can affect the transmissions of diseases. To supplement the findings of this study, basic reproduction numbers for the two patches were also determined. We found that the dispersal rate has profound effects on the transmission of infectious diseases since increase in the dispersal rate in one community an increases the disease transmission in the other and the opposite is also true. Therefore, the transmission of diseases in not severely affected communities can be contained when travel ban is imposed in the worst affected communities.

Keywords: Continuous-time Markov Chain; Epidemic Dispersal; Gillespie Algorithm; Basic Reproduction Number

INTRODUCTION

Access to relevant healthcare, described as an important social determinant of health, is essential in preventing many infectious diseases, including sexually transmitted diseases [1]. Studying disease transmission, along with problems of healthcare provisions, can provide additional insight into the population dynamic of the affected communities. Due to the lack of equity in accessing healthcare facilities, death rates from infectious diseases in developing countries exceed those from industrialized ones [2]. For example, a delay in containing the transmission of Ebola virus in West Africa was linked with high rates of poverty, as well as poor healthcare provisions [3]. Consequently, communicable diseases, such as measles, Covid-19 and Ebola virus, can be rapidly transmitted between communities with better healthcare facilities and others that lack those facilities. This can be possible through a connectivity, which was described as a key driver of epidemic dispersal, among those communities [4].

Since communicable diseases spread easily from one country to the other, epidemic patch models (5) remain the most suitable mathematical tools for describing such scenarios. Many interesting results are obtained from these models. For example, the susceptible-infected-recovered (SIR) model incorporating dispersal terms reported the transmission of diseases during migration between patches [6]. A deterministic susceptible-infected-susceptible (SIS) model suggested that the increase in reproduction number in any patches can intensify the spread of the disease therein [7]. The probability of disease extinction was estimated through a two-patch continuous-time Markov chain (CTMC) model for the transmission of *Salmon anaemia* virus [8].

Epidemic dispersal plays a vital role in understanding how pathogens are spreading among different patches, whose inhabitants can be either humans or animals (or both). This dispersal can be as a result of many factors, among which are global trades and variation in climatic patterns [9]. Epidemic dispersal has been studied using a verity of mathematical models, including classical systems like Kermack-Mckendir [10]. Another important model was the logistic growth dispersal, whose time component incorporates an inverse power law function [11]. This model, along with empirical data, estimates the initial epidemic outbreak, as well as the frequency of susceptible hosts. Due to the importance of disease dispersal in epidemiology, the effects of various dispersal mechanisms were investigated. For example, using an SIS model, the effects of dispersal on infected individuals was studied by examining both the long and short terms behaviour of the dispersal [12]. A verity of moment closures was used to study the effect of disease dispersal on epidemic threshold in plants [13]. This suggested that the disease transmission can be possible by the dispersal of pathogen. The effect of the initial condition of epidemic class on spatio-temporal pattern was examined through Cauchy distribution, which reported that the rate at which a disease increases per day can be influenced by the median dispersal distance [14]. The effects of the pathogen life cycle were studied, through a modified power law, which reported the strong influence of infectious period on epidemic dispersal [15]. The performance of different control strategies of foot and mouth epidemic was evaluated using the stochastic epidemic dispersal, through which both the history and the duration of epidemic were assessed [16].

When investigating the dynamics of epidemics, researchers often devised different mathematical models, depending on the problem under study. These include the deterministic and stochastic models. While the former deals with the formulations of ordinary differential equations (ODEs) to provide exact results [17], the later uses the probability of random events, often constructed through CTMC, to approximate the solutions of ODEs [18]. Compartmental models, formulated by ODEs, are useful in epidemiology; for example, they estimate epidemic persistence [19], through an important threshold called a basic reproduction number [20]. On the other hand, stochastic models are hard to be formulated; they are more informative [21]. Important findings in epidemiology, such as correlation between infected individuals [23], disease emergence and re-emergence [24] and extinction of diseases [20, 26], are reported through the computer simulations of stochastic models. Since the literature on modeling of epidemic dispersal involving healthcare facilities is lacking, this study combined both deterministic and stochastic approaches to address such a problem. We aim at investigating the effects of dispersal rates on diseases transmitting between two patches, whose inhabitants differed in healthcare provisions.

Community one lacks a recovery rate due to poor healthcare services, while the recovery rate is included in community two since they enjoy better healthcare facilities. The dynamic of an epidemic population due to changes in dispersal rates, together with the reproduction number, is examined through the stochastic and deterministic SIS models. We determined the basic reproduction number at the disease-free equilibrium using the next generation matrix. The distribution of the epidemic is estimated through the computer simulations of CTMC model.

Materials and Methods
Continuous Time Markov Chain model
Suppose that $S_1(t)$ and $S_2(t)$, each of which interacts with their corresponding infectious group $I_1(t)$ and $I_2(t)$, represent the population of two susceptible individuals inhabiting two different patches at time t. While the individuals in patch one lack a speedy recovery due to poor healthcare facilities therein, those in patch two enjoying better healthcare facilities are assumed to have some remarkable recovery from a spreading pathogen. Therefore, the CTMC of this process can be written as $\{S_1(t), I_1(t), S_2(t), I_2(t) : t \geq 0\}$, whereby $S_1(t), I_1(t), S_2(t)$ and $I_2(t)$ are the state spaces of the process, and t is the continuous-time representing the parameter space.

Given that population counts $S_1(t)$, $I_1(t)$, $S_2(t)$ and $I_2(t)$ take values m_1, m_2, m_3 and m_4, respectively, we write the probability mass function of the process as

$$p(m_1, m_2, m_3, m_4 : t) = p\big(S_1(t) = m_1, I_1(t) = m_2, S_2(t) = m3, I_2(t) = m_4\big), \quad (1)$$

where $m_1 = m_2 = m_3 = m_4 = 0,1,2,3,...$

To derive the mean-field equations, ODE model, capturing the dynamics of the spread of two pathogens in the two different patches, we write schematic reactions of the process as follows [27, 29]:

1. The two susceptible groups $S_1(t)$ and $S_2(t)$ can be infected by the infectious individuals $I_1(t)$ and $I_2(t)$ at the rates β_1 and β_2 respectively, such that

   $S_1(t) + I_1(t) \xrightarrow{\beta_1} 2I_1(t)$ and $S_2(t) + I_2(t) \xrightarrow{\beta_2} 2I_2(t)$.

2. Due to the provision of better healthcare facilities in patch two, some $I_2(t)$ can move to $S_2(t)$ class when infected at a recovery rate γ, such that

   $I_2(t) \xrightarrow{\gamma} S_2(t)$.

3. While susceptible individuals $S_1(t)$ can leave their favourable habitat (patch one) to another habitat (patch two) at a dispersal rate ρ_1, those in patch two can move to patch one at the rate ρ_2. These can be expressed as

   $S_1(t) \xrightarrow{\rho_1} S_2(t)$ and $S_2(t) \xrightarrow{\rho_2} S_1(t)$.

4. The infectious individuals inhabiting patch one $I_1(t)$ can move to patch two at ρ_1. Meanwhile, those infected in patch two can leave for patch one at the dispersal rate ρ_2. We present these as follows

   $I_1(t) \xrightarrow{\rho_1} I_2(t)$ and $I_2(t) \xrightarrow{\rho_2} I_1(t)$.

Considering all the events happening between the time interval $(t, t + \Delta t)$ (where Δt is an infinitesimal time), we write their transition rates, along with the corresponding changes, as follows.

Table 1: Transition rates for CTMC model of $S_1 I_1 S_2 I_2$ with dispersal

Event	Transition between t and $t + \Delta t$	Probability
i) $S_1(t)$ is infected by $I_1(t)$	$(m_1 + 1, m_2 - 1, m_3, m_4) \rightarrow (m_1, m_2, m_3, m_4)$	$\beta_1(m_1 + 1)(m_2 - 1)\Delta t + 0(\Delta t)^2$
ii) $S_2(t)$ is infected by $I_2(t)$	$(m_1, m_2, m_3 + 1, m_4 - 1) \rightarrow (m_1, m_2, m_3, m_4)$	$\beta_2(m_3 + 1)(m_4 - 1)\Delta t + 0(\Delta t)^2$
iii) $I_2(t)$ lost	$(m_1, m_2, m_3, m_4 + 1) \rightarrow (m_1, m_2, m_3, m_4)$	$\gamma(m_4 + 1)\Delta t + 0(\Delta t)^2$
iv) $S_2(t)$ recovered	$(m_1, m_2, m_3 - 1, m_4) \rightarrow (m_1, m_2, m_3, m_4)$	$\gamma(m_3 - 1)\Delta t + 0(\Delta t)^2$
v) $S_1(t)$ leaves patch one	$(m_1 + 1, m_2, m_3, m_4) \rightarrow (m_1, m_2, m_3, m_4)$	$\rho_1(m_1 + 1)\Delta t + 0(\Delta t)^2$
vi) $S_1(t)$ appears in patch two	$(m_1, m_2, m_3 - 1, m_4) \rightarrow (m_1, m_2, m_3, m_4)$	$\rho_1(m_3 - 1)\Delta t + 0(\Delta t)^2$
vii) $S_2(t)$ leaves patch two	$(m_1, m_2, m_3 + 1, m_4) \rightarrow (m_1, m_2, m_3, m_4)$	$\rho_2(m_3 + 1)\Delta t + 0(\Delta t)^2$
viii) $S_2(t)$ appears in patch one	$(m_1 - 1, m_2, m_3, m_4) \rightarrow (m_1, m_2, m_3, m_4)$	$\rho_2(m_1 - 1)\Delta t + 0(\Delta t)^2$
ix) $I_1(t)$ leaves patch one	$(m_1, m_2 + 1, m_3, m_4) \rightarrow (m_1, m_2, m_3, m_4)$	$\rho_1(m_2 + 1)\Delta t + 0(\Delta t)^2$
x) $I_1(t)$ appears in patch two	$(m_1, m_2, m_3, m_4 - 1) \rightarrow (m_1, m_2, m_3, m_4)$	$\rho_1(m_4 - 1)\Delta t + 0(\Delta t)^2$
xi) $I_2(t)$ leaves patch two	$(m_1, m_2, m_3, m_4 + 1) \rightarrow (m_1, m_2, m_3, m_4)$	$\rho_2(m_4 + 1)\Delta t + 0(\Delta t)^2$
xii) $I_2(t)$ appears in patch one	$(m_1, m_2 - 1, m_3, m_4) \rightarrow (m_1, m_2, m_3, m_4)$	$\rho_2(m_2 - 1)\Delta t + 0(\Delta t)^2$

When substituting the probabilities given in Table 1 into Equation (1) and taking the limit as the results approaches infinity, we obtain the following master equation [28]

$$\frac{dp(m_1, m_2, m_3, m_4; t)}{dt} = -p(m_1, m_2, m_3, m_4; t)(\beta_1 m_1 m_2 + \beta_2 m_1 m_2 + \gamma m_3 + \gamma m_4$$

$$+ \rho_1 m_1 + \rho_2 m_3 + \rho_2 m_3 + \rho_2 m_1 + \rho_1 m_2 + \rho_1 m_4 + \rho_2 m_4 + \rho_2 m_2)$$
$$+ p(m_1 + 1, m_2 - 1, m_3, m_4; t)\beta_1(m_1 + 1)(m_2 - 1)$$
$$+ p(m_1, m_2, m_3 + 1, m_4 - 1; t)\beta_2(m_3 + 1)(m_4 - 1)$$
$$+ p(m_1, m_2, m_3, m_4 + 1; t)\gamma(m_4 + 1) + p(m_1, m_2, m_3 - 1, m_4; t)\gamma(m_3 - 1)$$
$$+ p(m_1 + 1, m_2, m_3, m_4; t)\rho_1(m_1 + 1) + p(m_1, m_2, m_3 - 1, m_4; t)\rho_1(m_3 - 1)$$

$$+ p(m_1, m_2, m_3 + 1, m_4; t)\rho_2(m_3 + 1) + p(m_1 - 1, m_2, m_3, m_4; t)\rho_2(m_1 - 1)$$
$$+ p(m_1, m_2 + 1, m_3, m_4; t)\rho_1(m_2 + 1) + p(m_1, m_2, m_3, m_4 - 1; t)\rho_1(m_4 - 1)$$
$$+ p(m_1, m_2, m_3, m_4 + 1; t)\rho_2(m_4 + 1) + p(m_1, m_2 - 1, m_3, m_4; t)\rho_2(m_2 - 1) \quad (2)$$

Equation (2) can be simplified using the following probability generating function [21,22],

$$F(z_1, z_2, z_3, z_4; t) = \sum_{m_1}^{\infty}\sum_{m_2}^{\infty}\sum_{m_3}^{\infty}\sum_{m_4}^{\infty} p(m_1, m_2, m_3, m_4; t) z_1^{m_1} z_2^{m_2} z_3^{m_3} z_4^{m_4}. \quad (3)$$

Taking the derivative of Equation (3) with respect to *t*, we get

$$\frac{\partial F(z_1, z_2, z_3, z_4; t)}{\partial t} = \sum_{m_1}^{\infty}\sum_{m_2}^{\infty}\sum_{m_3}^{\infty}\sum_{m_4}^{\infty} \frac{dp(m_1, m_2, m_3, m_4; t)}{dt} z_1^{m_1} z_2^{m_2} z_3^{m_3} z_4^{m_4}. \quad (4)$$

Substituting Equation (2) into (4) and simplifying the result therein, we get the following equation [38]

$$\frac{\partial F(z_1, z_2, z_3, z_4; t)}{\partial t} = \beta_1 z_2 (z_2 - z_1)\frac{\partial^2 F(z_1, z_2, z_3, z_4; t)}{\partial z_1 z_2}$$
$$+ \beta_2 z_4 (z_4 - z_3)\frac{\partial^2 F(z_1, z_2 z_3, z_4; t)}{\partial z_3 z_4}$$
$$+ \gamma(1 - z_4)\frac{\partial F(z_1, z_2, z_3, z_4; t)}{\partial z_4} + \gamma z_3 (z_3 - 1)\frac{\partial F(z_1, z_2, z_3, z_4; t)}{\partial z_3}$$
$$+ \rho_1(1 - z_1)\frac{\partial(z_1, z_2, z_3, z_4; t)}{\partial z_1} + \rho_1 z_3 (z_3 - 1)\frac{\partial F(z_1, z_2, z_3, z_4; t)}{\partial z_3}$$
$$+ \rho_2(1 - z_3)\frac{\partial F(z_1, z_2, z_3, z_4; t)}{\partial z_3} + \rho_2 z_1 (z_1 - 1)\frac{\partial F(z_1, z_2, z_3, z_4; t)}{\partial z_1}$$
$$+ \rho_1(1 - z_2)\frac{\partial F(z_1, z, z_3, z_4; t)}{\partial z_2} + \rho_1 z_4 (z_4 - 1)\frac{\partial F(z_1, z, z_3, z_4; t)}{\partial z_4}$$
$$+ \rho_2(1 - z_4)\frac{\partial F(z_1, z, z_3, z_4; t)}{\partial z_4} + \rho_2 z_2 (z_2 - 1)\frac{\partial F(z_1, z, z_3, z_4; t)}{\partial z_2}. \quad (5)$$

The moment generating function defined by $M(\omega_1, \omega_2, \omega_3, \omega_4; t) = F(e^{\omega 1}, e^{\omega 2}, e^{\omega 3}, e^{\omega 4}; t)$ [30] can be used to simplify Equation (5) as follows

$$\frac{\partial M(\omega_1, \omega_2, \omega_3, \omega_4; t)}{\partial t} = \beta_1(e^{-\omega_1}e^{\omega_2} - 1)\frac{\partial^2 M(\omega_1, \omega_2, \omega_3, \omega_4; t)}{\partial\omega_1\partial\omega_2}$$
$$+ \beta_2(e^{-\omega_3}e^{\omega_4} - 1)\frac{\partial^2 M(\omega_1, \omega_2, \omega_3, \omega_4; t)}{\partial\omega_3\partial\omega_4}$$
$$+ \gamma(e^{-\omega_4} - 1)\frac{\partial M(\omega_1, \omega_2, \omega_3, \omega_4; t)}{\partial\omega_4} + \gamma(e^{\omega_3} - 1)\frac{\partial M(\omega_1, \omega_2, \omega_3, \omega_4; t)}{\partial\omega_3}$$
$$+ \rho_1(e^{-\omega_1} - 1)\frac{\partial M(\omega_1, \omega_2, \omega_3, \omega_4; t)}{\partial\omega_1} + \rho_1(e^{\omega_3} - 1)\frac{\partial M(\omega_1, \omega_2, \omega_3, \omega_4; t)}{\partial\omega_3}$$
$$+ \rho_2(e^{-\omega_3} - 1)\frac{\partial M(\omega_1, \omega_2, \omega_3, \omega_4; t)}{\partial\omega_3} + \rho_2(e^{\omega_1} - 1)\frac{\partial M(\omega_1, \omega_2, \omega_3, \omega_4; t)}{\partial\omega_1}$$
$$+ \rho_1(e^{-\omega_2} - 1)\frac{\partial M(\omega_1, \omega_2, \omega_3, \omega_4; t)}{\partial\omega_2} + \rho_1(e^{\omega_4} - 1)\frac{\partial M(\omega_1, \omega_2, \omega_3, \omega_4; t)}{\partial\omega_4}$$
$$+ \rho_2(e^{-\omega_4} - 1)\frac{\partial M(\omega_1, \omega_2, \omega_3, \omega_4; t)}{\partial\omega_4} + \rho_2(e^{\omega_2} - 1)\frac{\partial M(\omega_1, \omega_2, \omega_3, \omega_4; t)}{\partial\omega_2} \quad (6)$$

Using the notation $\frac{\partial^n M(0; t)}{\partial t} = \mathbb{E}(Z_i^n)$ for $i = 1, 2, 3, 4$ [38],

we calculate $\dfrac{\partial M(\omega_1,\omega_2,\omega_3,\omega_4;t)}{\partial \omega_i}\Big|_{\omega_i=0}$ from Equation (6) and present the results as follows:

$$\frac{d\mathbb{E}(z_1(t))}{dt} = -\beta_1 \mathbb{E}\big(z_1(t)z_2(t)\big) - \rho_1 \mathbb{E}\big(z_1(t)\big) + \rho_2 \mathbb{E}\big(z_1(t)\big) \tag{7a}$$

$$\frac{d\mathbb{E}(z_2(t))}{dt} = \beta_1 \mathbb{E}\big(z_1(t)z_2(t)\big) + \rho_2 \mathbb{E}\big(z_2(t)\big) + \rho_1 \mathbb{E}\big(z_2(t)\big) \tag{7b}$$

$$\frac{d\mathbb{E}(z_3(t))}{dt} = -\beta_2 \mathbb{E}\big(z_3(t)z_4(t)\big) - \gamma \mathbb{E}\big(z_3(t)\big) - \rho_2 \mathbb{E}\big(z_3(t)\big) + \rho_1 \mathbb{E}\big(z_3(t)\big) \tag{7c}$$

$$\frac{d\mathbb{E}(z_4(t))}{dt} = \beta_2 \mathbb{E}\big(z_3(t)z_4(t)\big) - \gamma \mathbb{E}\big(z_4(t)\big) - \rho_2 \mathbb{E}\big(z_4(t)\big) + \rho_1 \mathbb{E}\big(z_4(t)\big) \tag{7d}$$

Considering condition (2) stated in the schematic reactions, we assume that $\gamma\, E(Z_3(t)) \approx \gamma\, E(Z_4(t))$ in Equation (7c). Other assumptions can be made from condition (3) as $\rho_2\, E(Z_1(t)) \approx \rho_2\, E(Z_3(t))$ in Equation (7a), and $\rho_1\, E(Z_3(t)) \approx \rho_1\, E(Z_1(t))$ in Equation (7c). Meanwhile, condition (4) assumes that $\rho_2\, E(Z_2(t)) \approx \rho_2\, E(Z_4(t))$ in Equation (7b), and $\rho_1\, E(Z_4(t)) \approx \rho_1\, E(Z_2(t))$ in Equation (7d). Applying these changes on Equations (7a,7b,7c and 7d), we write

$$\frac{d\,\mathbb{E}(Z_1(t))}{dt} = -\beta_1\,\mathbb{E}(Z_1(t)Z_2(t)) - \rho_1\,\mathbb{E}(Z_1(t)) + \rho_2\,\mathbb{E}(Z_3(t))$$
$$\frac{d\,\mathbb{E}(Z_2(t))}{dt} = \beta_1\,\mathbb{E}(Z_1(t)Z_2(t)) - \rho_1\,\mathbb{E}(Z_2(t)) + \rho_2\,\mathbb{E}(Z_4(t))$$
$$\frac{d\,\mathbb{E}(Z_3(t))}{dt} = -\beta_2\,\mathbb{E}(Z_3(t)Z_4(t)) + \gamma\,\mathbb{E}(Z_4(t)) - \rho_2\,\mathbb{E}(Z_3(t)) + \rho_1\,\mathbb{E}(Z_1(t))$$
$$\frac{d\,\mathbb{E}(Z_4(t))}{dt} = \beta_2\,\mathbb{E}(Z_3(t)Z_4(t)) - \gamma\,\mathbb{E}(Z_4(t)) - \rho_2\,\mathbb{E}(Z_4(t)) + \rho_1\,\mathbb{E}(Z_2(t)). \tag{8}$$

A heuristic approach allows us to write these equations as follows

$$\frac{dS_1(t)}{dt} = -\beta_1 S_1(t)I_1(t) - \rho_1 S_1(t) + \rho_2 S_2(t)$$
$$\frac{dI_1(t)}{dt} = \beta_1 S_1(t)I_1(t) - \rho_1 I_1(t) + \rho_2 I_2(t)$$
$$\frac{dS_2(t)}{dt} = -\beta_2 S_2(t)I_2(t) + \gamma I_2(t) - \rho_2 S_2(t) + \rho_1 S_1(t)$$
$$\frac{dI_2(t)}{dt} = \beta_2 S_2(t)I_2(t) - \gamma I_2(t) - \rho_2 I_2(t) + \rho_1 I_1(t). \tag{9}$$

Equation (9), the system of ODEs, represents the SIS compartments of two different infectious groups spreading pathogens in their corresponding susceptible populations, inhabiting two different patches. While the individuals in patch one do not recover (on time) after contracting the disease, those in patch two would remarkably recover due to the availability of better healthcare facilities therein. The model Equation (9), whose all parameters are assumed to be positive, did not capture the birth of new individuals, as well as their natural mortality.

Basic Reproduction Number, R_0

The basic reproduction number, denoted by the symbol R_o, can be used to measure the spread of disease in a given population [19]. If $R_o < 1$, few infected individuals interacts with the susceptible community, through which the epidemic would fail to spread. Meanwhile, if $R_o > 1$ increases the number of infected individuals. This is an indication that the disease would spread rapidly [36].

Playing vital roles in understanding many epidemiological problems such as disease outbreaks [34] and extinctions [33], the basic reproduction number can be estimated through different mathematical formulations [32]. Thus, in this study, R_o is determined by linearising the system of ODEs Equation (9) about disease-free equilibrium [37]. Two matrices F, containing all rates of secondary infections, and V, whose elements are recovery and transfer rates, are estimated from the disease compartments of the ODEs as follows: $F = \begin{bmatrix} \beta_1 & 0 \\ 0 & \beta_2 \end{bmatrix}$ and $V = \begin{bmatrix} \rho_1 & -\rho_2 \\ -\rho_1 & \gamma + \rho_2 \end{bmatrix}$.

Following the determination of the spectral radius $\rho(K) = FV^{-1}$, through the computation of the eigenvalues of the product FV^{-1}, we get the two basic reproduction numbers of the system Equation (9) as follows:

$$R_{o1} = \frac{\beta_1\rho_2 + \beta_2\rho_1 + \gamma\beta_1 + \eta}{2\rho_1\gamma} \tag{10}$$

and

$$R_{o2} = \frac{\beta_1\rho_2 + \beta_2\rho_1 + \gamma\beta_1 - \eta}{2\rho_1\gamma}, \tag{11}$$

whereby $\eta = \sqrt{\beta_1^2\rho_2^2 + 2\beta_1^2\rho_2\gamma + \beta_1^2\gamma^2 + 2\beta_1\beta_2\rho_1\rho_2 - 2\beta_1\beta_2\rho_1\gamma + \beta_2^2\rho_1^2}$.

One should note that R_{01} is the basic reproduction number of a community with poor healthcare facilities, while that of a community enjoying better healthcare facilities is given as R_{02}.

It can be easily shown that $\eta > 0$ for all $\beta_1,\beta_2,\gamma,\rho_1,\rho_2 \geq 0$. Thus, from Equations (10) and (11) $R_{o2} < R_{o1}$. This signifies that the introduction of a recovery term, in a community with better healthcare facilities, would suppress a pathogen spreading therein.

RESULTS AND DISCUSSION

Numerical Examples

In order to determine the effects of dispersal rates on the populations of two infectious classes $I_1(t)$ and $I_1(t)$, inhabiting two different patches, two mathematical approaches, CTMC and ODE models, are implemented. The ODE model Equation (9) can be simply solved numerically through the MATLAB ODE solver, ode45. Meanwhile, since the master equation (2) can be difficult to solve, the Gillespie algorithm [35] is employed to numerically solve the formulation of CTMC. This method uses two random numbers, r_1 and r_2, generated from the uniform distribution. While r_1 estimates the inter-event time, r_2 updates the continuous-time in the process [38]. For example, if the probability of any events of interest is less than r_1, the population count of this event is to be increased by one. This process continuous until all the listed events are exhausted. The time would be updated accordingly.

The effects of epidemic dispersal can be determined by holding other parameters of the model, β_1, β_2 and γ, constant and varying the values of dispersal rates ρ_1 and ρ_2. This allows us to examine the changes in the population of infectious classes, through stochastic realisations and trajectories of the solution of ODE model Equation (9). For example, when the values of two dispersal rates are the

same ($\rho_1 = \rho_2 = 0.05$), the difference in the population sizes of the infectious classes $I_1(t)$ and $I_2(t)$ is only due to the disparity in their transmission rates, as well as the recovery rate included in the compartment of $I_2(t)$ (see Figure 1). When considering the population of susceptible individuals, we found that $S_1(t) < S_2(t)$, while the difference in the two basic reproduction numbers was found to be $R_{02} < R_{01}$ (Figure 1).
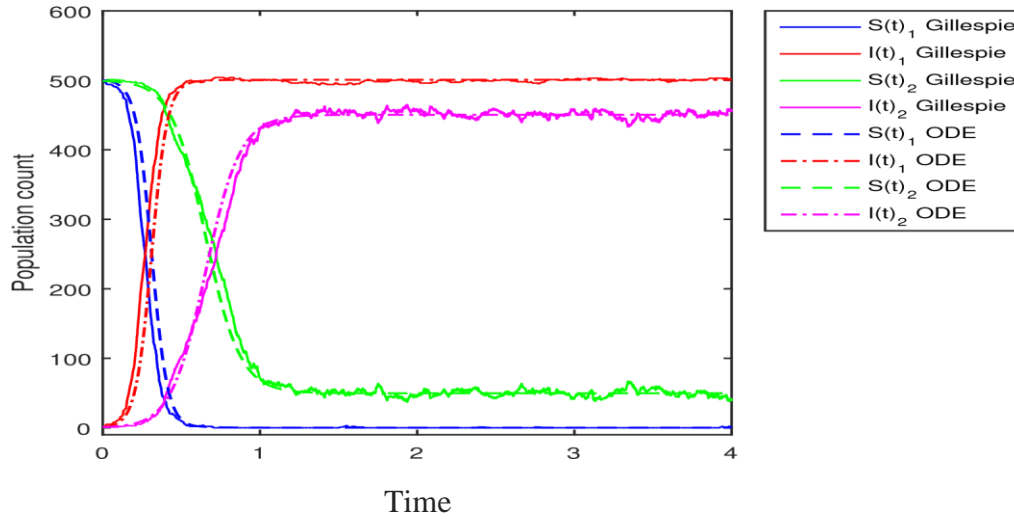

Figure 1: When the values of dispersal rates are the same $\rho_1 = \rho_2$, the change in population counts of the two infectious classes $I_1(t)$ and $I_2(t)$ is only due to differences in transmission and recovery rates. Both the solution of ODE and Gillespie realisation are estimated at $\beta_1 = 0.04$, $\beta_2 = 0.02$, $\gamma = 1$, $\rho_1 = \rho_2 = 0.05$, $S_1(0) = 500$, $S_2(0) = 499$, $I_1(0) = 1$, $I_2(0) = 1$, $R_{01} = 0.8410$ and $R_{02} = 0.0190$.

When the dispersal rate of the infectious class $I_1(t)$ is more than that of $I_2(t)$ ($\rho_1 = 0.3$, $\rho_2 = 0.03$), the population size of $I_2(t)$ increases (see Figure 2). We found that $S_1(t) < S_2(t)$, and $R_{02} < R_{01}$ (Figure 2). One should note that other parameters of the model are also kept constant, as reported previously.
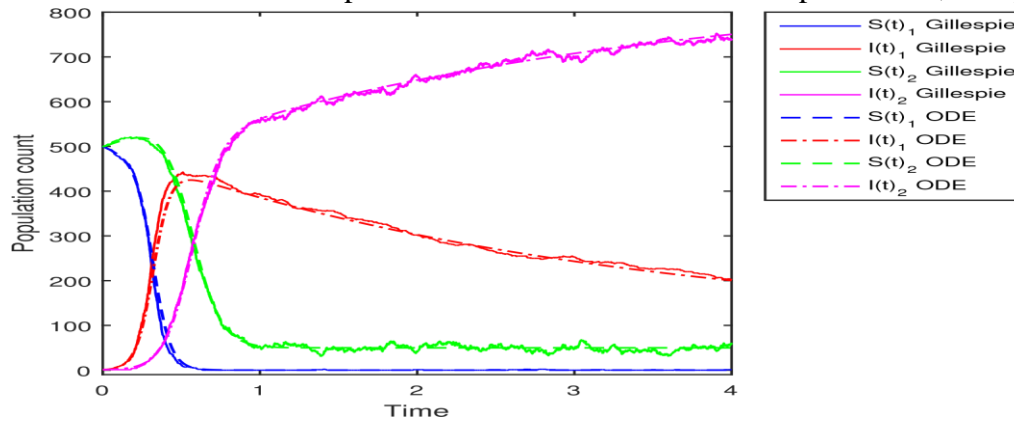

Figure 2: When $\rho_1 > \rho_2$, the population count of $I_2(t)$ increases. One Gillespie realization, along with the solution of corresponding ODEs, is estimated at $\beta_1 = 0.04$, $\beta_2 = 0.02$, $\gamma = 1$ $\rho_1 = 0.3$, $\rho_2 = 0.03$, $S_1(0) = 500$, $S_2(0) = 499$, $I_1(0) = 1$, $I_2(0) = 1$, $R_{01} = 0.1380$ and $R_{02} = 0.0193$.

Moreover, the transmission rates β_1 and β_2, together with the recovery rate γ, are still kept constant. However, the dispersal rates are varied to determine the difference in the population counts of the two infectious classes, $I_1(t)$ and $I_2(t)$. This technique is similar to that of the previous result. When $\rho_2 > \rho_1$ ($\rho_1 = 0.05, \rho_2 = 0.5$), the population of the infectious class $I_1(t)$ increases (see Figure (3)). We also found that the population count of susceptible class $S_2(t)$ is greater than that of $S_1(t)$, while the basic reproduction R_{02} is still less than R_{01}.
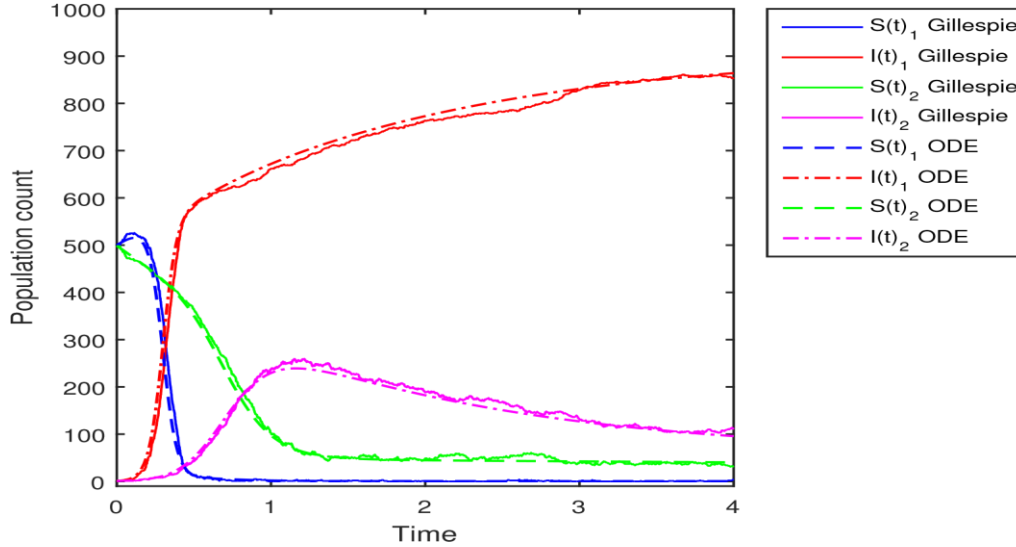

Figure 3: When $\rho_2 > \rho_1$, the population count of $I_1(t)$ increases. One Gillespie realization approximates the solution of the corresponding ODEs for $\beta_1 = 0.04$, $\beta_2 = 0.02$, $\gamma = 1$ $\rho_1 = 0.05$, $\rho_2 = 0.5$, $S_1(0) = 500$, $S_2(0) = 499$, $I_1(0) = 1$, $I_2(0) = 1$, $R_{01} = 1.2067$ and $R_{02} = 0.0133$.

Since Figures 1, 2 and 3 report the differences in population sizes of infectious classes $I_1(t)$ and $I_2(t)$ through one realisation of Gillespie algorithm, these differences are further investigated by performing 1000 simulations. Maintaining values of transmission and recovery rates, as well as the initial number of population sizes, similar to those reported in the previous results, the distributions of $I_1(t)$ and $I_2(t)$ are estimated at $t = 2$ (Figure 2). When $\rho_1 = \rho_2 = 0.05$, the mean and variance of $I_1(t)$ are slightly more than those obtained in $I_2(t)$ (Figure 4 (a),(b)). Varying the values of the dispersal rates to $\rho_1 > \rho_2$ ($\rho_1 = 0.3, \rho_2 = 0.03$), the mean and variance of $I_2(t)$ grow higher (see Figure 4 (c),(d)). However, when the dispersal rates are changed to $\rho_2 > \rho_1$ ($\rho_1 = 0.05, \rho_2 = 0.5$), the mean and the variance of infectious class $I_1(t)$ increase rapidly (Figure 4 (e),(f)).
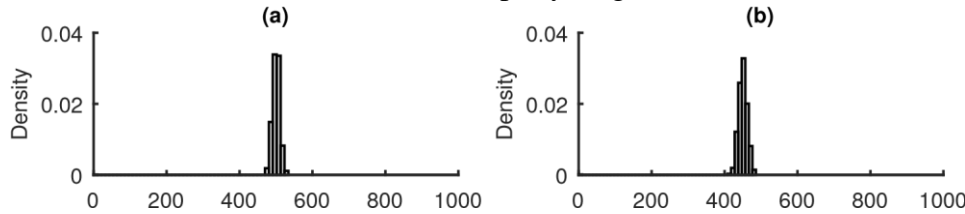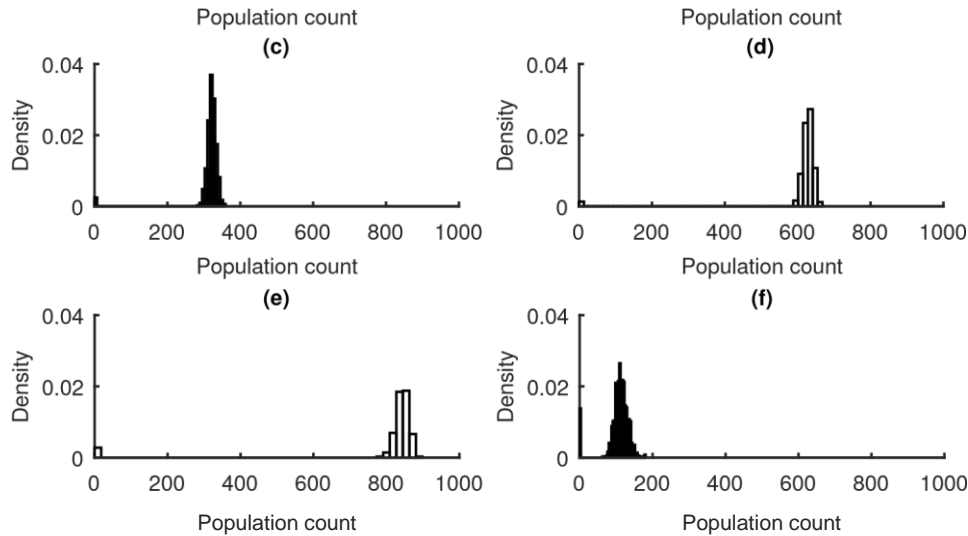
Figure 4: Increase in the dispersal rate in one patch increases the number of infectious individuals in the other. The distributions of population counts for $I_1(t)$ and $I_2(t)$ are estimated through 1000 Gillespie realisations (sample paths) at $t = 2$. (a) and (b) are obtained using the parameters of Figure 1, (b) and (c) are estimated by the parameters of Figure 2, and (d) and (e) are approximated through thJe parameters of Figure 3. (a) and (b) are respectively the distributions of $I_1(t)$ and $I_2(t)$ for $\rho_1 = \rho_2$; (c) and (d) are respectively the distributions of $I_1(t)$ and $I_2(t)$ for $\rho_1 > \rho_2$; (e) and (f) are respectively the distributions of $I_1(t)$ and $I_2(t)$ for $\rho_2 > \rho_1$. While the mean and variance of $I_1(t)$ in (a) are $\mu = 499.96$ and $\sigma^2 = 593.57$, those of $I_2(t)$ in (b) are $\mu = 450.00$ and $\sigma^2 = 347.00$, respectively. The mean and variance of $I_1(t)$ in (c) are $\mu = 316.52$ and $\sigma^2 = 1.96 \times 10^3$ whereas those of $I_2(t)$ in (d) are $\mu = 616.91$ and $\sigma^2 = 7.15 \times 10^3$, respectively. The mean and variance of $I_1(t)$ in (e) are $\mu = 801.78$ and $\sigma^2 = 3.41 \times 10^4$ while those of $I_2(t)$ in (f) are $\mu = 108.54$ and $\sigma^2 = 899.78$, respectively.

The effects of dispersal rates on the population of individuals inhabiting two patches, differed in healthcare provisions, are studied through the stochastic SIS model, along with its deterministic counterpart. It was assumed that community one do not recover (on time) to the spreading disease due to poor healthcare facilities. Meanwhile, the provision of better healthcare facilities in community two conferred recovery to the individuals therein. Our finding suggests that the CTMC model, devised through the computer simulation of Gillespie method, approximates the compartmental ODE model Equation (9). This was true in all the results reported in this study despite the fact that the dispersal rates were varied when examining their effects on the population of infected individuals (see Figures 1,2 and 3). Other studies [24, 18, 34], dealt with different scenarios, also reported similar to this finding.

Through the dynamics of epidemic dispersal in two different communities are considered in the same system, the study suggests that the disease can be easily contained in the community with better healthcare facilities compared to the other that lacks those facilities. This was reported through the comparison of basic reproduction numbers for the population of two different communities (see Figures 1,2 and 3). This finding, properly described by our model, is expected since the recovery rate was included in the community with better healthcare provisions.

The effects of dispersal rates on disease transmission are studied by comparing the number of infected individuals in the two communities. The finding of this study suggests that increase in the dispersal rate in one community increases the population of infected individuals in the other. Also, decrease in dispersal rate in one community decreases the number of infected individuals in the other community (Figures 2,3 and 4). This is possible since the transmission of infectious diseases, through transportation, was reported in many studies [13, 6]. It is clear that a disease transmission does not only depend on transmission rates, but also on the dispersal rates. Incorporated in the model, dispersal rates have profound effects on the population counts of infectious classes. Thus, this study suggests that the transmission of infectious diseases, to other communities, would be easily contained if the rate of movement of individuals in the affected communities is reduced.

CONCLUSION

This study suggests that the dispersal rates have profound effects on the transmission of infectious diseases between two different communities. Therefore, the spread of diseases can be easily contained by restricting the movement of individuals, through imposing travel ban and other related measures, to not seriously affected communities. Since it takes a longer time to apply other control measures, such as vaccination strategies, in containing transmissions of most epidemic diseases, this study, conducted using modelling approach, gives additional insight into the existing problem. Though the mathematical derivations, as well the computer simulations, considered only two patches, this can be extended to three or more depending on a problem needs to be addressed. Further studies, including the evaluation of different control strategies and the computation of probability of epidemic extinctions, can be conducted on spatial epidemic dispersal modelling.

References

1. Hogben H, & Leichliter. JS. Social determinants and sexually transmitted disease disparities. *Sexually transmitted diseases*, pages 2008: S13–S18.
2. Yudkin JS, Holt RIG, Silva-Matos, C, & Beran D. Twinning for better diabetes care: a model for improving healthcare for non-communicable diseases in resource-poor countries, 2009.
3. Fallah, MP, Skrip, LA, Gertler S, Dan Yamin D, & Galvani AP. Quantifying poverty as a driver of ebola transmission. *PLoS Neglected Tropical Diseases*, 9(12):e0004260, 2015.
4. Kraemer MUG, Hay SI, Pigott DM, Smith DL, Wint GRW, & Golding N. Progress and challenges in infectious disease cartography. *Trends in Parasitology*, 2016:32(1), 19–29.
5. Bichara D, Kang Y, Castillo-Chavez C, Horan R, & Perrings C. Sis and sir epidemic models under virtual dispersal. *Bulletin of Mathematical Biology*, 2015:77, 2004–2034.
6. Wendi Wang W, & Zhao X-Q. An epidemic model with population dispersal and infection period. *SIAM Journal on Applied Mathematics*, 2006: 66(4), 1454–1472.
7. Wendi Wang & Xiao-Qiang Zhao. An epidemic model in a patchy environment. *Mathematical biosciences*, 2004: 190(1), 97–112.
8. Milliken E. The probability of extinction of infectious salmon anemia virus in one and two patches. *Bulletin of Mathematical Biology*, 2017:79(12), 2887–2904.

9. Fabre F, Coville J, & Cunniffe NJ. Optimising reactive disease management using spatially explicit models at the landscape scale. In *Plant Diseases and Food Security in the 21st Century*, pages 47–72. Springer, 2021.

10. Yang F-Y, Li Y, Li W-T, & Wang Z-C. Traveling waves in a nonlocal dispersal kermack-mckendrick epidemic model. *Discrete & Continuous Dynamical Systems-Series B*, 2013:18(7).

11. Mundt CC, Sackett KE, Wallace LD, Cowger C, & Dudley JP. Aerial dispersal and multiple-scale spread of epidemic disease. *EcoHealth*,2009: 6:546–552.

12. Filipe JAN, & Maule MM. Effects of dispersal mechanisms on spatio-temporal development of epidemics. *Journal of Theoretical Biology*, 2004:226(2):125–141.

13. Brown DH, & Bolker BM. The effects of disease dispersal and host clustering on the epidemic threshold in plants. *Bulletin of Mathematical Biology*, 2004: 66:341–371.

14. Xu X-M, & Ridout MS. Effects of initial epidemic conditions, sporulation rate, and spore dispersal gradient on the spatio-temporal dynamics of plant disease epidemics. *Phytopathology*, 1998:88(10):1000–1012.

15. Sackett KE, & Mundt CC. The effects of dispersal gradient and pathogen life cycle components on epidemic velocity in computer simulations. *Phytopathology*, 2005:95(9):992–1000.

16. Keeling MJ, Woolhouse MEJ, Shaw DJ, Matthews L, Chase-Topping M, Haydon DT, Cornell SJ, Kappey J, Wilesmith J, & Grenfell TB. Dynamics of the 2001 Uk foot and mouth epidemic: stochastic dispersal in a heterogeneous landscape. *Science*, 2001:294(5543):813–817.

17. Hurtado PJ. Building new models: Rethinking and revising ode model assumptions. *An Introduction to Undergraduate Research in Computational and Mathematical Biology: From Birdsongs to Viscosities*, pages 1–86, 2020.

18. Allen LJS. A primer on stochastic epidemic models: Formulation, numerical simulation, and analysis. *Infectious Disease Modelling*, 2017: 2(2),128–142.

19. Driessche PV, & Yakubu A. Disease extinction versus persistence in discrete-time epidemic models. *Bulletin of Mathematical Biology*, 81(11), 4412– 4446.

20. Liang X, Lei Zhang L, & Zhao X-Q. Basic reproduction ratios for periodic abstract functional differential equations (with application to a spatial model for lyme disease). *Journal of Dynamics and Differential Equations*, 2019: 31, 1247–1278.

21. Kot M. *Elements of mathematical ecology*. Cambridge University Press, 2001.

22. Grimmett G, & Stirzaker D. *Probability and random processes*. Oxford University Press, 2020.

23. Meakin SR, & Keeling MJ. Correlations between stochastic epidemics in two interacting populations. *Epidemics*, 2019:26, 58–67.

24. Nandi A, & Allen LJS. Stochastic two-group models with transmission dependent on host infectivity or susceptibility. *Journal of Biological Dynamics*, 2019:13(sup1), 201–224.

25. Liu Q, Jiang D, Hayat T, & Alsaedi A. Dynamics of a stochastic multigroup siqr epidemic model with standard incidence rates. *Journal of the Franklin Institute*, 2019:356(5):2960–2993.

26. Montagnon P. A stochastic sir model on a graph with epidemiological and population dynamics occurring over the same time scale. *Journal of Mathematical Biology*, 2019:79:31–62.

27. McKane AJ, & Newman TJ. Predator-prey cycles from resonant amplification of demographic stochasticity. *Physical Review Letters*, 2005:94(21), 218102.

28. Black AJ & McKane AJ. Stochastic formulation of ecological models and their applications. *Trends in Ecology & Evolution*, 2012:27(6):337–345.

29. Erban R, Chapman J, & Maini P. A practical guide to stochastic simulations of reaction-diffusion processes. *arXiv preprint arXiv:* 2007:0704.1908.

30. Bailey NTJ. *The elements of stochastic processes with applications to the natural sciences*, volume 25. John Wiley & Sons, 1991.

31. Brauer F, Van den Driessche P, Wu J, & Allen LJS. *Mathematical epidemiology*, volume 1945. Springer, 2008.

32. Delamater PL, Street EJ, Leslie TF, Yang YT, & Jacobsen KH. Complexity of the basic reproduction number (r0). *Emerging Infectious Diseases*, 2019:25(1), 1.

33. Brightwell G, House T, & Luczak M. Extinction times in the subcritical stochastic sis logistic epidemic. *Journal of Mathematical Biology*, 2018:77, 455–493.

34. Lahodny GE, & Allen LJS. Probability of a disease outbreak in stochastic multipatch epidemic models. *Bulletin of Mathematical Biology*, 2013:75, 1157–1180.

35. Gillespie DT. Exact stochastic simulation of coupled chemical reactions. *The Journal of Physical Chemistry*,1977:81(25), 2340–2361.

36. Allen LJS, Wesley CL, Owen RD, Goodin DG, Koch D, Jonsson CB, Chu Y-K, Hutchinson JMS, & Paige RL. A habitat-based model for the spread of hantavirus between reservoir and spillover species. *Journal of Theoretical Biology*, 2009: 260(4), 510–522.

37. Lewis MA, Renclawowicz J, van den Driessche P, & Wonham M. A comparison of continuous and discrete-time west Nile virus models. *Bulletin of Mathematical Biology*, 2006:68, 491–509.

38. Linda JS Allen. *An introduction to stochastic processes with applications to biology*. CRC press, 2010.